Atmospheric Research 247 (2021) 105212

Contents lists available at ScienceDirect

Atmospheric Research

journal homepage: www.elsevier.com/locate/atmosres

Links between the thermal condition of the Tibetan Plateau in summer and atmospheric circulation and climate anomalies over the Eurasian continent

Sulan Nan*, Ping Zhao*, Junming Chen, Ge Liu

State Key Laboratory of Severe Weather, Chinese Academy of Meteorological Sciences, Beijing 100081, China

ARTICLE INFO

Keywords:
Thermal condition of the Tibetan Plateau
Tropospheric temperature gradient
Eurasian westerly jet
Asian climate

ABSTRACT

We examine the links between the thermal condition of the troposphere over the Tibetan Plateau with the atmospheric circulation and climate over the Eurasian continent. The temperature of the troposphere over the Tibetan Plateau is higher than the temperature in other regions at the same latitude and is consistent with the temperature of the Eurasian troposphere on an interannual timescale. The higher temperature of the troposphere over the Tibetan Plateau leads to anomalous south–north temperature gradients from mid-latitudes over the Eurasian continent to its two flanks, accompanied by anomalous easterly and westerly winds in the upper troposphere in the subtropics and at higher latitudes. Anomalous anticyclonic circulations and subsidence motions appear between the anomalous easterly and westerly winds and contribute to the high surface air temperature over West Asia, Central Asia and East Asia via anomalous vertical temperature advection in the troposphere and change in the amount of solar radiation incident on the surface. The enhanced East Asian summer monsoon associated with the high temperature of the troposphere over the Tibetan Plateau also partly contributes to the high surface air temperature over East Asia via horizontal temperature advection. The westerly wind anomalies in the north of the mid-latitudes over the Eurasian continent indicate the enhancement and northward shift of the mid-latitude westerly jet. This is related to anomalous upward motion and higher precipitation in Northeast China and North China. Sensitivity experiments based on an atmospheric model verify the impact of anomalous tropospheric heating over the Tibetan Plateau in summer on the atmospheric circulation over the Eurasian continent.

1. Introduction

The Tibetan Plateau is the highest plateau in the world and has remarkable dynamic and thermodynamic effects on the atmospheric circulation in Asia (Ye and Gao, 1979; Wu et al., 1997). The blocking effect of the Tibetan Plateau in the boreal winter forces the mid-latitude westerly jet stream to diverge and form northern and southern branches (Yeh, 1950). The surface sensible heat over the Tibetan Plateau in spring drives ascending motion locally and modulates the Asian–Australian monsoon (Wu et al., 1997). In summer, the Tibetan Plateau acts as a source of heat and heating of the atmosphere over this vast elevated region affects the evolution of the Asian summer monsoon, the monsoon climate in East Asia and South Asia, and the desert climate of Central Asia (e.g. Luo and Yanai, 1984; Yanai et al., 1992; Zhang et al., 2004; Duan and Wu, 2005). The snow cover over the Tibetan Plateau, as a source of external forcing, is regarded as a sensitive indicator of the climate in South Asia and East Asia on interannual and interdecadal timescales (e.g., Ose, 1996; Robock et al., 2003; Zhang et al., 2004; Zhu et al., 2015; Wang et al., 2017). Precipitation over northwestern China before the rainy season, summer precipitation over the Yangtze River valley and the extent of the *mei-yu* are all closely related to the winter–spring snow cover on the Tibetan Plateau (Chen and Wu, 2000; Qin et al., 2006; Wu and Qian, 2003; Wang et al., 2017).

The Tibetan Plateau not only has an impact on the climate in the Asian monsoon region, but also remotely modulates the atmospheric circulation and climate in other areas. The physical mechanism of this remote influence is mainly through large-scale teleconnections and planetary/Rossby waves. Branstator, 2002 and Zhao et al. (2007) proposed that low-frequency disturbances and thermal anomaly of the Tibetan Plateau can propagate energy outward in the form of planetary waves along the westerly jet and connect with the extratropical atmospheric circulation. Nan et al. (2009) showed that the springtime tropospheric temperature anomaly over the Tibetan Plateau can cause anomalous winds over the tropical central-western Pacific and change the sea surface temperature over the tropical central-eastern Pacific via a teleconnection between Asia and the north Pacific Ocean. Lin and Wu

* Corresponding authors.
E-mail addresses: nansl@cma.gov.cn (S. Nan), zhaop@cma.gov.cn (P. Zhao).

https://doi.org/10.1016/j.atmosres.2020.105212
Received 9 January 2020; Received in revised form 20 August 2020; Accepted 20 August 2020
Available online 26 August 2020

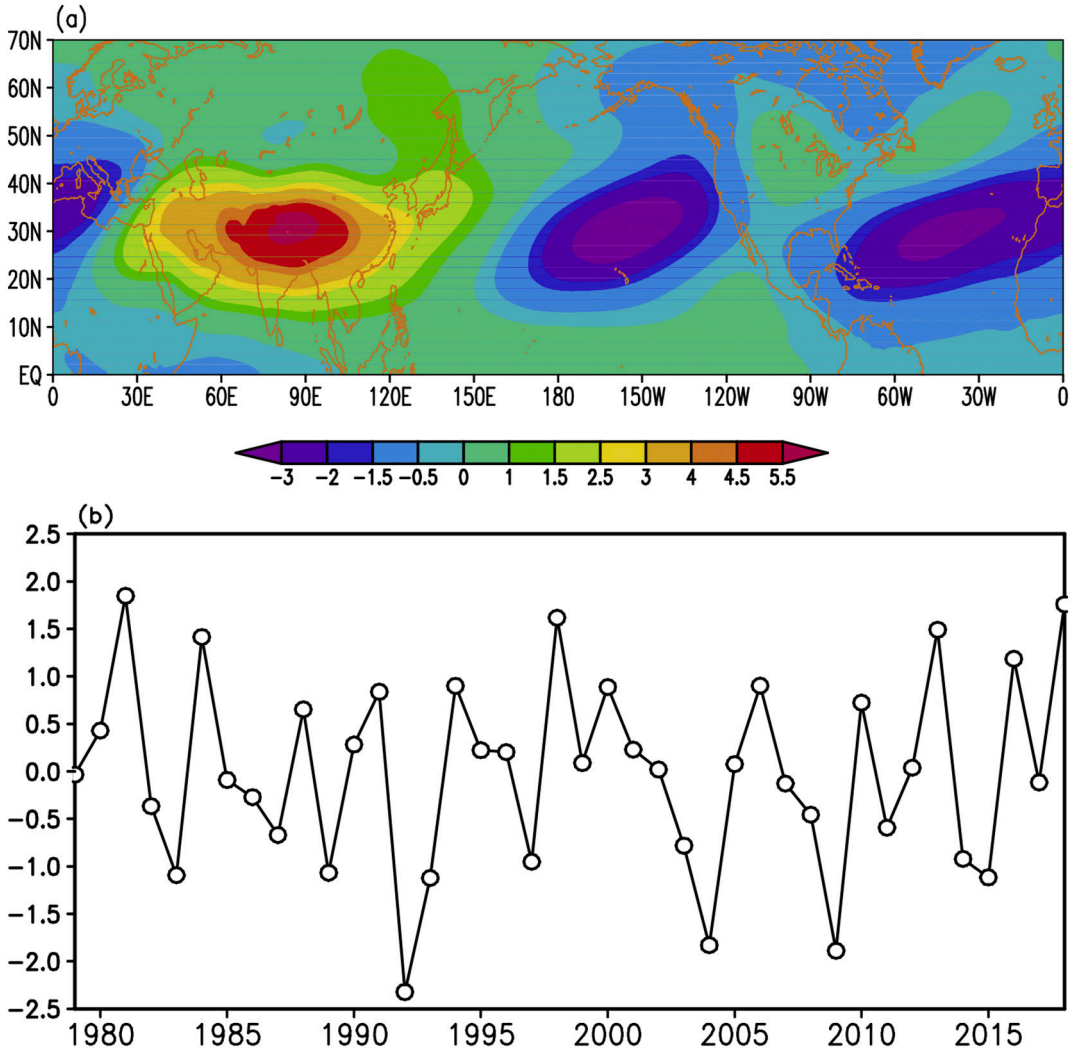

Fig. 1. (a) Climatology of the JJA vertically (500–200 hPa) averaged eddy air temperature (°C) (the difference of the air temperature from its zonal mean) during the time period 1979–2018. (b) Time series of the normalized and detrended JJA TTT index (the vertically (500–200 hPa) and regionally (25°N–45°N, 65°E–105°E) averaged air temperature) during the time period 1979–2018.

(2011) showed that the variability of snow cover over the Tibetan Plateau in the preceding autumn is significantly correlated with the winter surface air temperature (SAT) over North America via the Pacific–North America teleconnection. Wu et al. (2016) showed that anomalies in the snow cover on the Tibetan Plateau can trigger a teleconnection pattern across the Eurasian continent, leading to summer heatwaves in southern Europe and northeastern Asia.

The remote atmospheric circulation associated with the heating of the Tibetan Plateau not only involves large-scale teleconnections and the planetary/Rossby wave response, but also a uniform tropospheric temperature response over the Eurasian continent. Zhao et al. (2012) showed that anomalies in the Asian tropospheric temperature can propagate westward and lead to a uniform change in the tropospheric temperature in the Atlantic–Eurasian region. Recent studies have shown a uniform change in the tropospheric temperature at the same latitude as the Tibetan Plateau over the Eurasian continent related to the heating over the Tibetan Plateau (Lu et al., 2018; Nan et al., 2019).

This study focuses on the response of the uniform tropospheric temperature over the Eurasian continent to the Tibetan Plateau heating and examines the corresponding atmospheric circulation and climate over the Eurasian continent. The remainder of the paper is as follows. Section 2 describes the datasets, methodology and model used in this study. Section 3 presents the variation in the Tibetan tropospheric temperature (TTT) and its relationship with Eurasian atmospheric circulation and climate. Section 4 further investigates the atmospheric responses to the heating of the Tibetan Plateau and Section 5 presents our conclusion and discussion.

2. Data, methodology and model

We use the 1979–2018 European Centre for Medium-Range Weather Forecasts (ECMWF) interim reanalysis dataset (ERA-Interim; Simmons et al., 2007) with a 0.75° × 0.75° resolution. The variables include the surface pressure, surface downward solar radiation flux, medium and low cloud cover, air temperature, vertical velocity, and zonal and meridional winds. The SAT is obtained from the NASA Goddard Institute for Space Studies (GISS) dataset on a 2.0° × 2.0° global grid. The 160 station monthly precipitation and SAT datasets (1979–2018) in China are also used.

Correlation and composite analyses are used to detect the relation between the thermal condition of the Tibetan Plateau and the atmospheric circulation and climate over the Eurasian continent. Student's *t*-test is used to assess the statistical significance of the results of the composite and correlation analysis. Unless specified, the 95% confidence level is used to highlight significant signals. We concentrate on the analysis of the results averaged over the boreal summer months

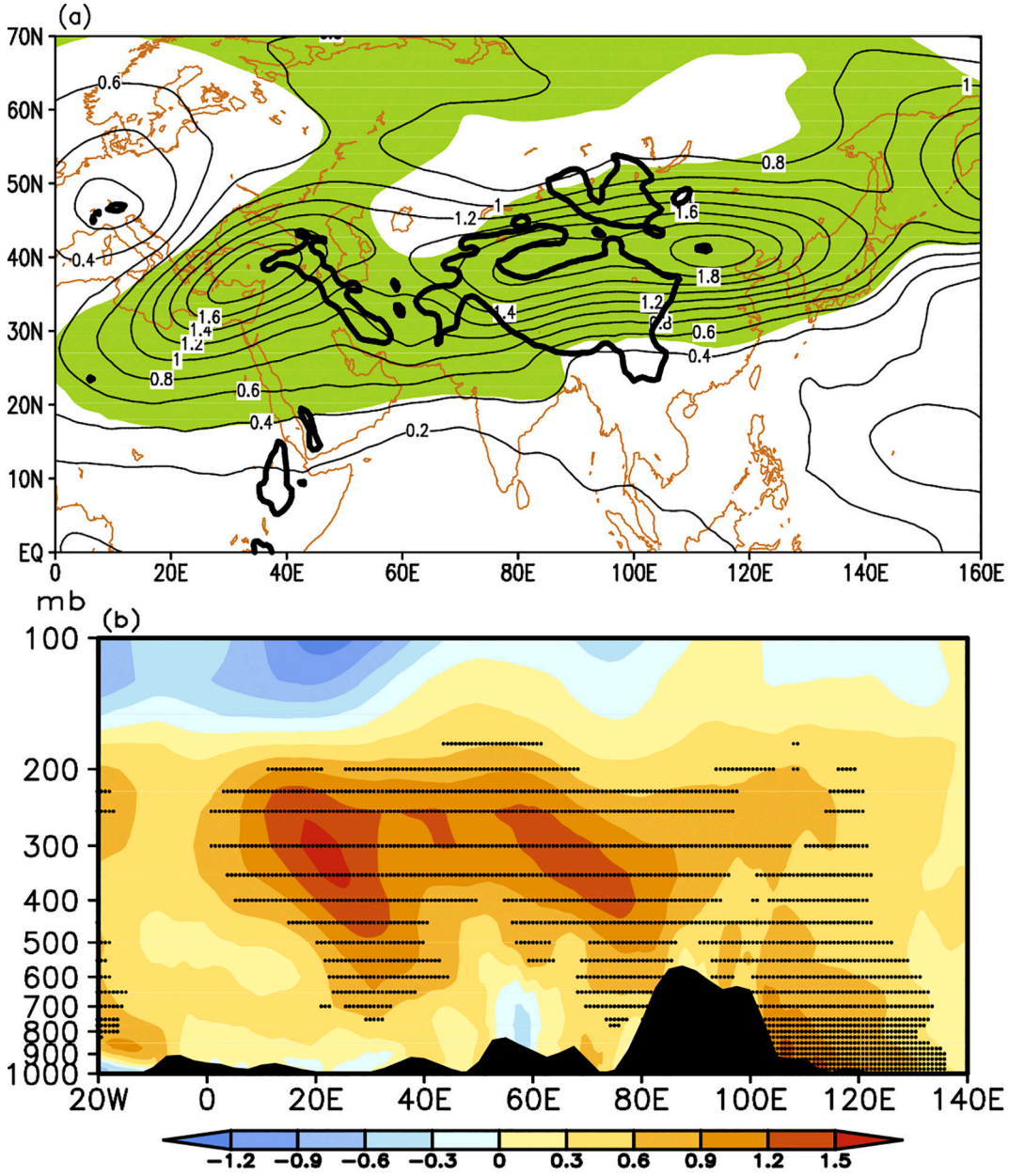

Fig. 2. Composite differences in (a) the vertically averaged (500–200 hPa) air temperature (°C) and (b) the air temperature (°C) along 30° N between the high and low TTT index cases. The thick and black line in part (a) represents the 1500 m topographic contour. The black shaded areas in part (b) indicate the topography. The shaded areas in part (a) and the stippled areas in part (b) are significant at the 95% confidence level.

(June–July–August, JJA).

The National Center for Atmospheric Research Community Atmospheric Model, version 3 (CAM3) (Collins et al., 2004) is used to assess the impact of heating by the Tibetan Plateau. CAM3 uses a T42 grid and has 26 vertical levels. The sea surface temperature scheme is set as the climatology with the annual cycle included.

We change the TTT with the CAM3 model by adjusting the type of vegetation. The climate–vegetation relationship is commonly separated into (1) the effect of climate on vegetation and (2) the effect of vegetation on climate (Cai et al., 2014, 2015). However, vegetation can also be used to force an atmospheric model. A change in the type of vegetation can lead to variations in atmospheric heating through the adjustment of the albedo of the vegetation (Zhao et al., 2012; Nan et al., 2019). We therefore carry out two numerical experiments with the CAM3 model: CAM3-tree and CAM3-bare. In CAM3-tree, the type of surface vegetation at each grid point within the Tibetan Plateau (i.e. above 1500 m) is set to 'broadleaf evergreen tropical tree'. The CAM3-bare experiment is the same as CAM3-tree except that the type of surface vegetation at each grid point within the Tibetan Plateau is set to 'not vegetated'. The differences between CAM3-tree and CAM3-bare are used to examine the impact of a thermal condition anomaly of the Tibetan Plateau on the atmospheric circulation over the Eurasian continent. The two experiments are integrated for 20 years. To avoid spin-up in the numerical experiments, only the last 10 years are used in our analysis.

3. Relation of TTT with the atmospheric circulation and climate over the Eurasian continent

3.1. Tropospheric temperature over the Tibetan Plateau/Eurasian continent

Relative to the oceans, continents are a source of heat in the summer

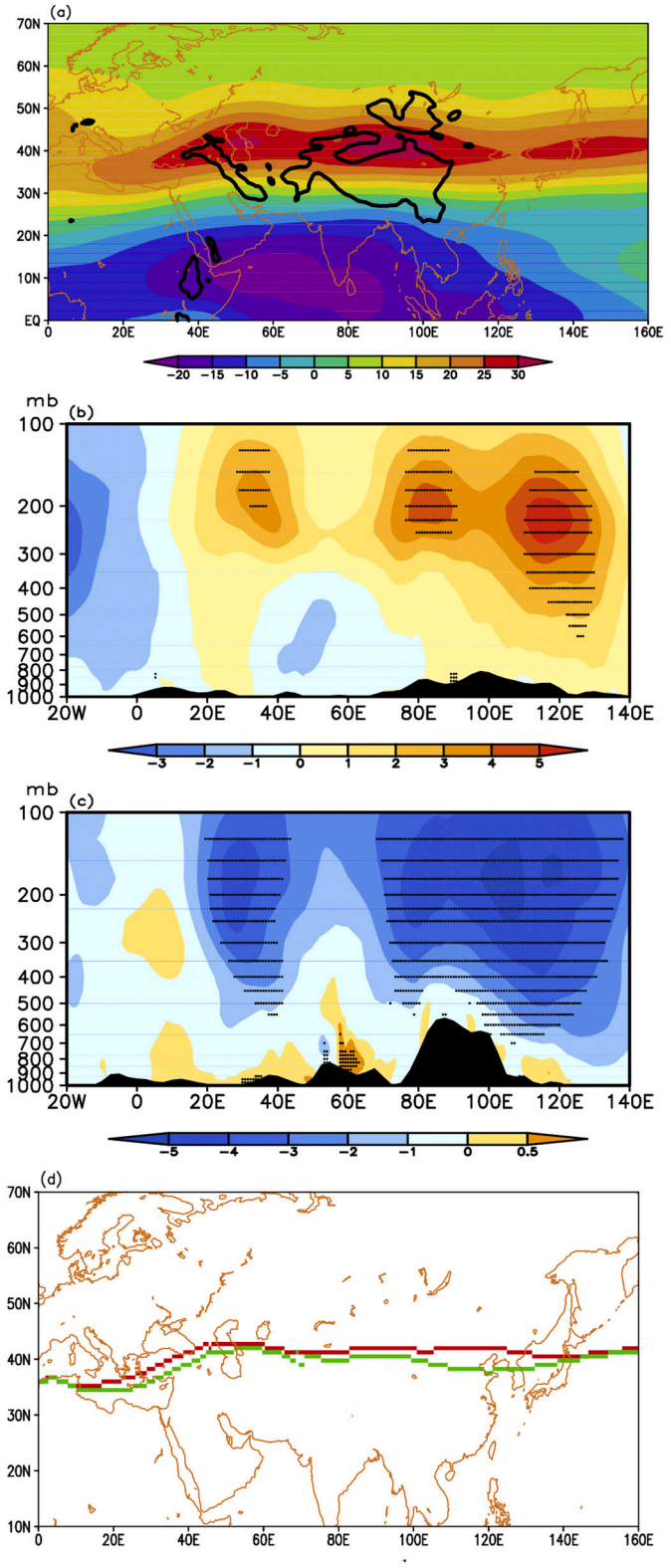

Fig. 3. (a) Climatology of the JJA zonal wind ($m \cdot s^{-1}$) during the time period 1979–2018. (b) Composite difference in the zonal wind ($m \cdot s^{-1}$) along 45° N between the high and low TTT index cases. (c) Composite difference in the zonal wind ($m \cdot s^{-1}$) along 30° N between the high and low TTT index cases. (d) The axes of the westerly jet in the high (red) and low (green) TTT index cases. The thick and black line in part (a) represents the 1500 m topographic contour. The black shaded areas in parts (b) and (c) indicate the topography and the stippled areas are significant at the 95% confidence level.

months. Eurasia is the largest continent and the Tibetan Plateau is the highest plateau. As a result, the heating effect of the Tibetan Plateau is important in the boreal summer. Fig. 1a shows the climatology of the vertically averaged (500–200 hPa) eddy tropospheric air temperature (the difference in air temperature from the zonal mean) calculated for the time period 1979–2018 (Fig. 1a). The highest eddy temperature is seen over the Eurasian continent, with the center over the Tibetan Plateau, indicating that the TTT is the highest tropospheric temperature at this latitude. This result is consistent with the work of Zhao et al. (2010). The heating of the Tibetan Plateau mainly comes from the surface sensible heat and condensation heating associated with the Asian monsoon and orographically forced rainfall (Liu et al., 2001, 2004). The tropospheric temperature reflects this heating synthesis. Therefore, consistent with the work of Nan et al. (2019), we use the TTT index to measure tropospheric thermal condition of the Tibetan Plateau.

The TTT index is calculated using the vertically (500–200 hPa) and regionally (25°N–45°N, 65°E–105°E; with the region approximately above the 1500-m topographic altitude) averaged air temperature during summer. The time series of the TTT index shows a clear interannual variation and a significant upward trend of 0.23 °C/10 years (> 95% confidence level) from 1979 to 2018. Because we focus on the relationship between the thermal condition of the Tibetan Plateau and the atmospheric circulation over the Eurasian continent on an interannual timescale, the TTT index is detrended (Fig. 1b). Unless specified, the trends of other variables are also removed in this study.

To detect variations in the distribution of the tropospheric temperature and the atmospheric circulation related to the interannual variability of the TTT from a composite analysis, we select the seven highest and lowest TTT index years on the basis of the JJA TTT index (Fig. 1b). The years with the highest TTT index are 1981, 1984, 1998, 2006, 2013, 2016, and 2018 (the high TTT index cases) and the years with the lowest TTT index (the low TTT index cases) are 1983, 1989, 1992, 1993, 2004, 2009, and 2015.

Fig. 2a shows the composite difference in the 500–200 hPa air temperature between the high and low TTT index cases. Significant positive anomalies appear at mid-latitudes over the Eurasian continent (MEC) between 20°N-50°N, with centers in West Asia, East Asia and Northeast Asia, indicating an increase in the MEC tropospheric temperature associated with a high TTT index. The correlation analysis of the detrended JJA TTT index with the 500–200 hPa tropospheric temperature over the Eurasian continent indicates a similar result (not shown). In the longitude–height cross-section of air temperature along 30° N (Fig. 2b), significant positive anomalies appear in the mid- to upper troposphere, spanning East Asia, Central Asia and West Asia. These results indicate that the tropospheric heating of the Tibetan Plateau is not isolated in summer and is of a similar nature to Eurasian tropospheric heating on an interannual timescale. These results are in agreement with those of Zhao et al. (2010) and Nan et al. (2019).

3.2. Linkage of the change of TTT with atmospheric circulation anomalies over the Eurasian continent

The positive MEC temperature anomaly in Fig. 2 implies anomalous meridional temperature gradients between the MEC and its two flanks. Based on thermal wind theory, the anomalous temperature gradient from mid-latitudes to the subtropics is accompanied by negative vertical shear between the upper and lower tropospheric zonal geostrophic winds (Nan et al., 2019). To the north of the MEC, the anomalous meridional thermal gradient between the MEC and higher latitudes implies positive vertical shear between the upper and lower tropospheric zonal geostrophic winds and an enhanced Eurasian westerly jet. Previous studies have also shown the close relation between the Eurasian westerly jet and the contrast in temperature between the MEC and higher latitudes. Zhang et al. (2006) reported that the seasonal evolution of the Eurasian westerly jet is associated with the meridional

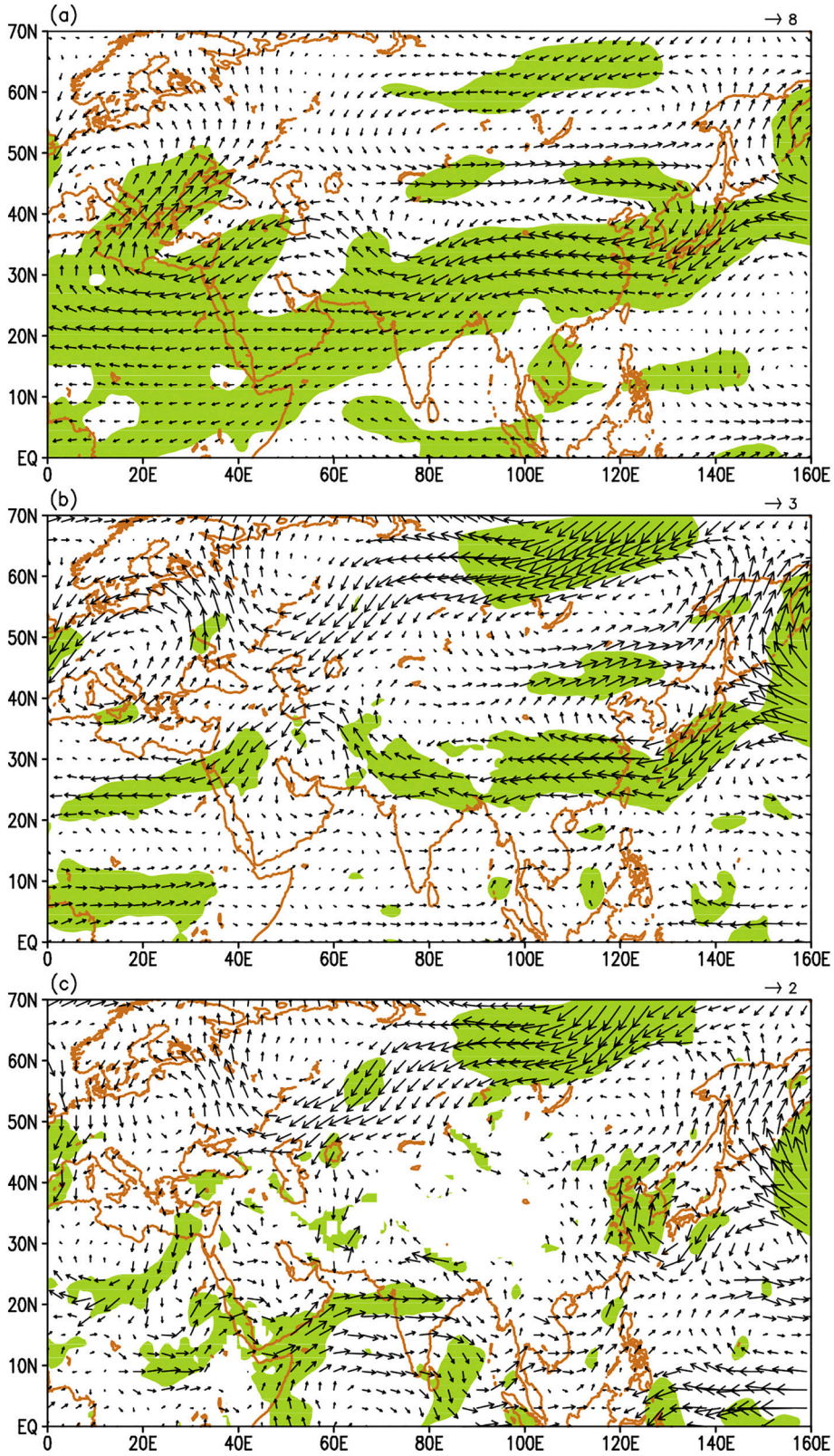

Fig. 4. Composite differences in the (a) 200, (b) 500 and (c) 850 hPa horizontal wind vectors ($m \cdot s^{-1}$) between the high and low TTT index cases. The shaded areas in parts (a–c) are significant at the 95% confidence level. The white areas over land in part (c) are the regions below the surface.

temperature contrast in the upper troposphere over the Eurasian continent. Subsequent studies have tied the intensity and meridional shift in the westerly jet to heating by the Tibetan Plateau and the temperature contrast between the Tibetan Plateau and the higher latitudes of Eurasia (Kuang and Zhang, 2005; Zhang et al., 2019). We investigate the relation between the change of TTT and the Eurasian westerly jet.

Fig. 3a shows the climatology (1979–2018) of the JJA 200 hPa zonal winds. In the boreal summer, the strong westerly flow—that is,

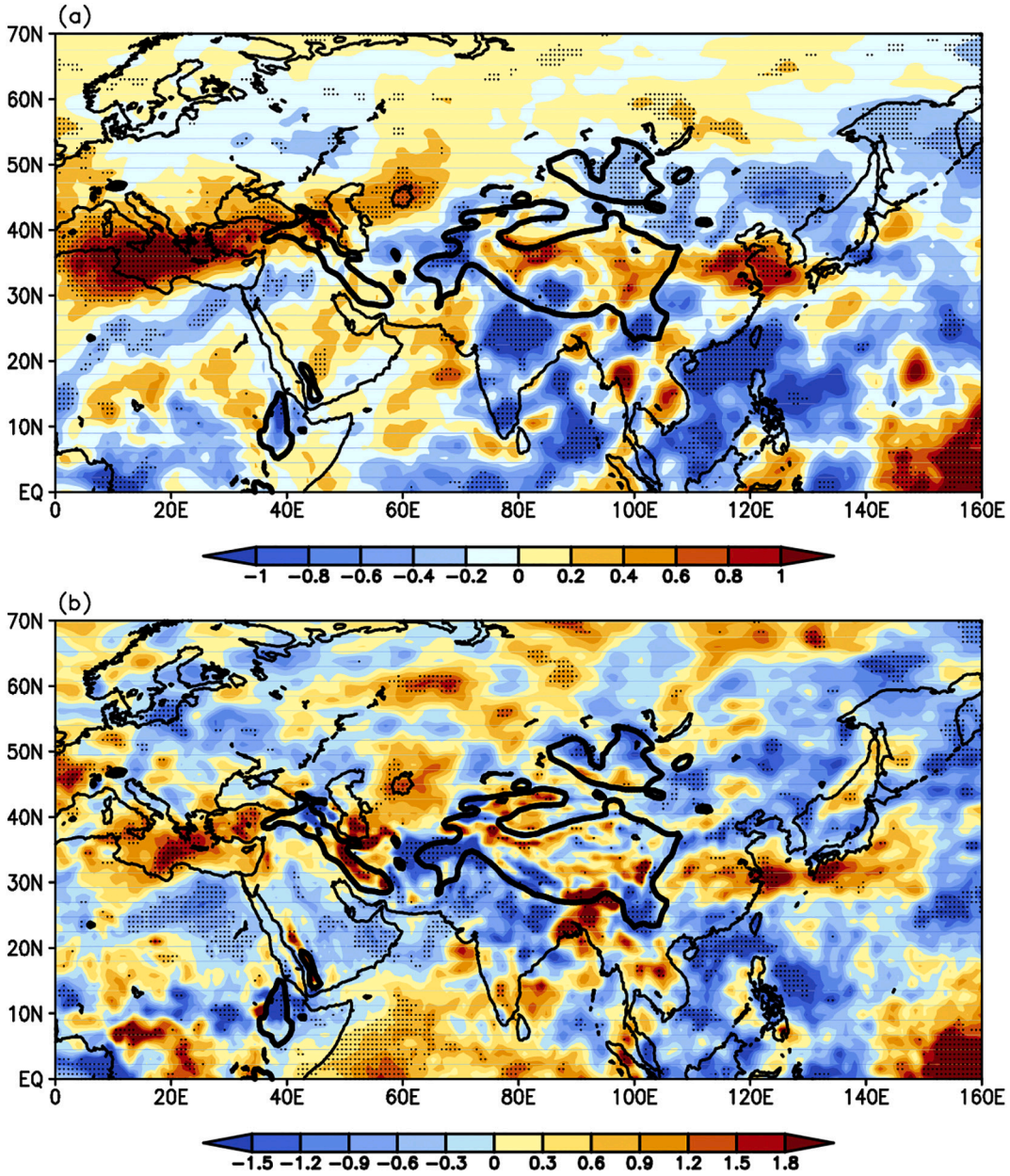

Fig. 5. Composite differences in the (a) 200 and (b) 500 hPa vertical velocities (10^{-2}·Pa·s^{-1}) between the high and low TTT index cases. The thick black lines represent the 1500 m topographic contour and the stippled areas are significant at the 90% confidence level.

the Eurasian westerly jet—prevails over the mid- to high latitudes of the Eurasian continent, with a maximum wind speed > 30 m/s near 40° N. The Tibetan Plateau is located on the southern flank of the westerly jet in summer.

Fig. 3b shows the longitude–height cross-section of the composite difference in the zonal winds along 45° N. There are significant positive anomalies (weak negative anomalies) in the mid- to upper (lower) troposphere. The positive vertical shear of the zonal winds between the upper and lower troposphere is in accord with the anomalous tropospheric temperature gradient from the MEC to the north (Fig. 2a) and indicates an enhancement of the westerly jet.

Fig. 3c shows the longitude–height cross-section of the composite difference in the zonal winds along 30° N. Significant negative anomalies appear in the mid- to upper troposphere, indicating weakening of the westerly winds in the mid- to lower latitudes of the Eurasian continent and in agreement with the anomalous tropospheric temperature gradient from the MEC to the south. The enhancement of the westerly winds at mid- to high latitudes and the weakening of the westerly winds at mid- to low latitudes imply a northward shift in the westerly jet. Fig. 3d shows the axes of the westerly jet in the high and low TTT index cases. The axis of the westerly jet shifts further north in the high TTT index cases than in the low TTT index cases, especially in West Asia and East Asia.

These features are also seen in the horizontal wind fields. Fig. 4a shows the composite difference in the 200 hPa horizontal wind field between the high and low TTT index cases. Anomalous easterly and westerly winds blow over the Eurasian continent at latitudes 25°N-35°N and 40°N-50°N, respectively, supporting the enhancement and northward shift of the Eurasian westerly jet. Anticyclonic circulations appear between the anomalous easterly and westerly winds, centered over West Asia near (35° N, 30° E), Central Asia near (40° N, 80° E) and East Asia near (40° N, 120° E) (Fig. 4a). The anomalous anticyclonic circulations over East Asia and Central Asia also can be seen in the mid-troposphere (Fig. 4b), with the centers slightly to the south relative to

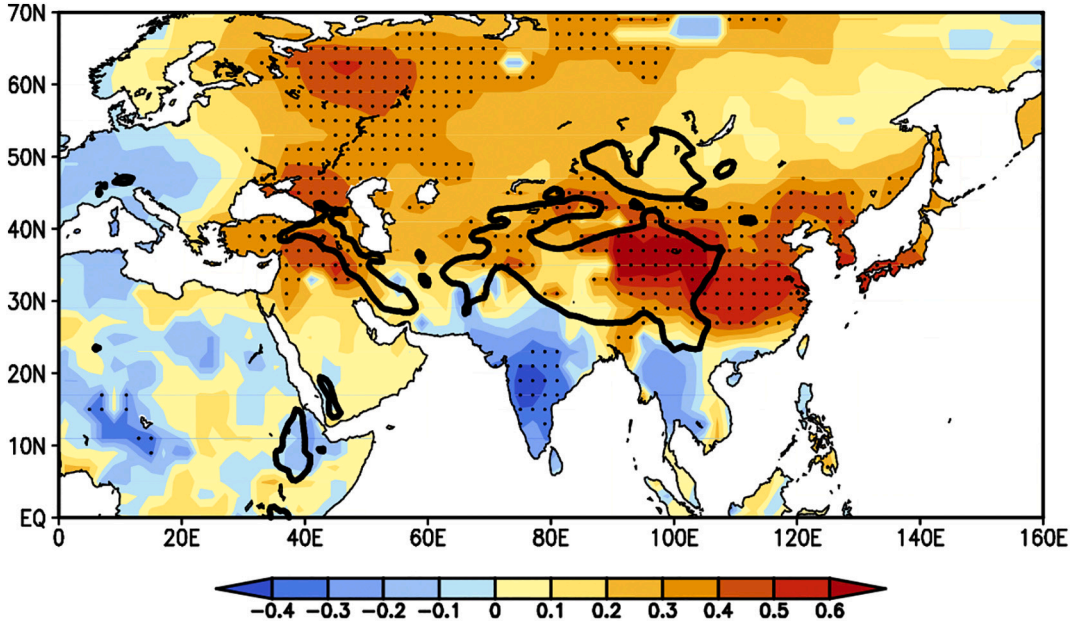

Fig. 6. Map of the correlation between the JJA TTT index and the GISS SAT during the time period 1979–2018. The thick black line represents the 1500 m topographic contour and the stippled areas are significant above the 95% confidence level.

those at 200 hPa. West Asia underlies the southern extension of an anomalous anticyclonic circulation centered at about (60° N, 50° E) at 500 hPa. There are anomalous cyclonic circulations over the Indochina Peninsula, the Indian Peninsula, and northern Africa to the south of the anomalous easterly winds over the MEC. This anomalous feature differs remarkably from the atmospheric circulation to the north of the anomalous easterly winds. At 850 hPa (Fig. 4c), an airflow blows over East Asia from the western Pacific and South China Sea toward mainland China, with the prevalence of southerly winds over South China, North China, and Northeast China, indicating an enhanced East Asian summer monsoon. Consistent with the anomalous anticyclonic circulation in the mid- to upper troposphere over the MEC (Fig. 4a and b), anomalous subsiding motion appears over West Asia, Central Asia and East Asia (Fig. 5).

3.3. Linkage of the change of TTT with climate anomalies over the Eurasian continent

The anomalous anticyclonic circulation and subsiding motion associated with a high TTT may cause the climate anomaly over the Eurasian continent. Previous studies have shown that anticyclonic circulation favors high-pressure blocking and is related to heatwaves (e.g., Namias, 1991; Galarneau et al., 2012; Drouard and Woollings, 2018). Fig. 6 shows the correlation map between the JJA TTT index and the GISS SAT during the time period 1979–2018. Significant positive correlations appear over West Asia, Central Asia and East Asia and correspond to the anomalous anticyclonic circulation and subsiding motion in mid-latitudes (Figs. 4 and 5). Negative correlations appear over the subtropics to the south of the anomalous easterly winds (Fig. 4b), especially over south Asia. Significant positive and weak negative correlations between the JJA TTT index and the SAT appear at mid-latitudes and in the subtropics over the Eurasian–African region, respectively. The positive–negative demarcation line is along the anomalous easterly winds (Fig. 4a and b). This result connects the thermal condition of the Tibetan Plateau to the SAT over the Eurasian continent. The anomalies in the meridional temperature gradients from the MEC to the north and south, associated with the high TTT, contribute to the anomalous anticyclonic circulation and subsiding motion over the mid- to high latitudes of Eurasia and the high SAT over West Asia, Central Asia and East Asia.

To further clarify the physical processes responsible for the linkage between the JJA TTT and the SAT over West Asia, Central Asia and East Asia, we calculate the heat budget anomalies in terms of thermodynamic equation:

$$\frac{1}{P_s - P_t}\int_{P_t}^{P_t}\left[-V_h\cdot\nabla T + \omega\left(\kappa\frac{T}{P} - \frac{\partial T}{\partial P}\right) + \frac{Q}{C_p}\right]dp = \frac{1}{P_s - P_t}\int_{P_t}^{P_t}\frac{\partial T}{\partial t}dp$$

Where V_h is the horizontal wind, ω is the vertical velocity, Q is non-adiabatic heating, T is temperature, P is air pressure,P_s is the lower boundary (here, the surface pressure), P_t the upper boundary (here, 100 hPa), C_p is specific heat of dry air at constant pressure, κ is the ratio of gas constant to specific heat at constant pressure. Fig. 7a presents the composite difference in horizontal temperature advection vertically integrated from the surface to 100 hPa between the high and low TTT index cases. Significant positive values appear over East Asia (northern China), indicating that the horizontal temperature advection anomaly associated with the high TTT contributes to the local increase in the SAT. This is mainly due to the enhanced East Asian summer monsoon (Fig. 4c), which transports a high-temperature air flow to northern China. The high SAT over East Asia (northern China) is therefore associated with the high TTT results from the horizontal temperature advection anomaly caused by the enhanced East Asian summer monsoon. Only small-area significant positive anomalies appear over the regions in Central Asia and West Asia with significant positive correlations between the JJA TTT index and the SAT, indicating that there is only a limited contribution of horizontal temperature advection to the high SAT over Central Asia and West Asia.

Fig. 7b shows the composite difference in the vertical temperature advection vertically integrated from the surface to 100 hPa between the high and low TTT index cases. Significant positive anomalies contributing to the high SAT appear in East Asia (the Yangtze River–Yellow River region), Central Asia, and West Asia. Combined with the anomalous subsiding motion over East Asia, Central Asia and West Asia (Fig. 5), we suggest that the relation between the JJA TTT and the SAT over East Asia (the Yangtze River–Yellow River region), Central Asia, and West Asia is partly due to the vertical temperature advection anomaly caused by the anomalous subsiding motion over these regions.

The anomalous subsiding motion associated with the high TTT (Fig. 5) also results in the change in non-adiabatic heating in these

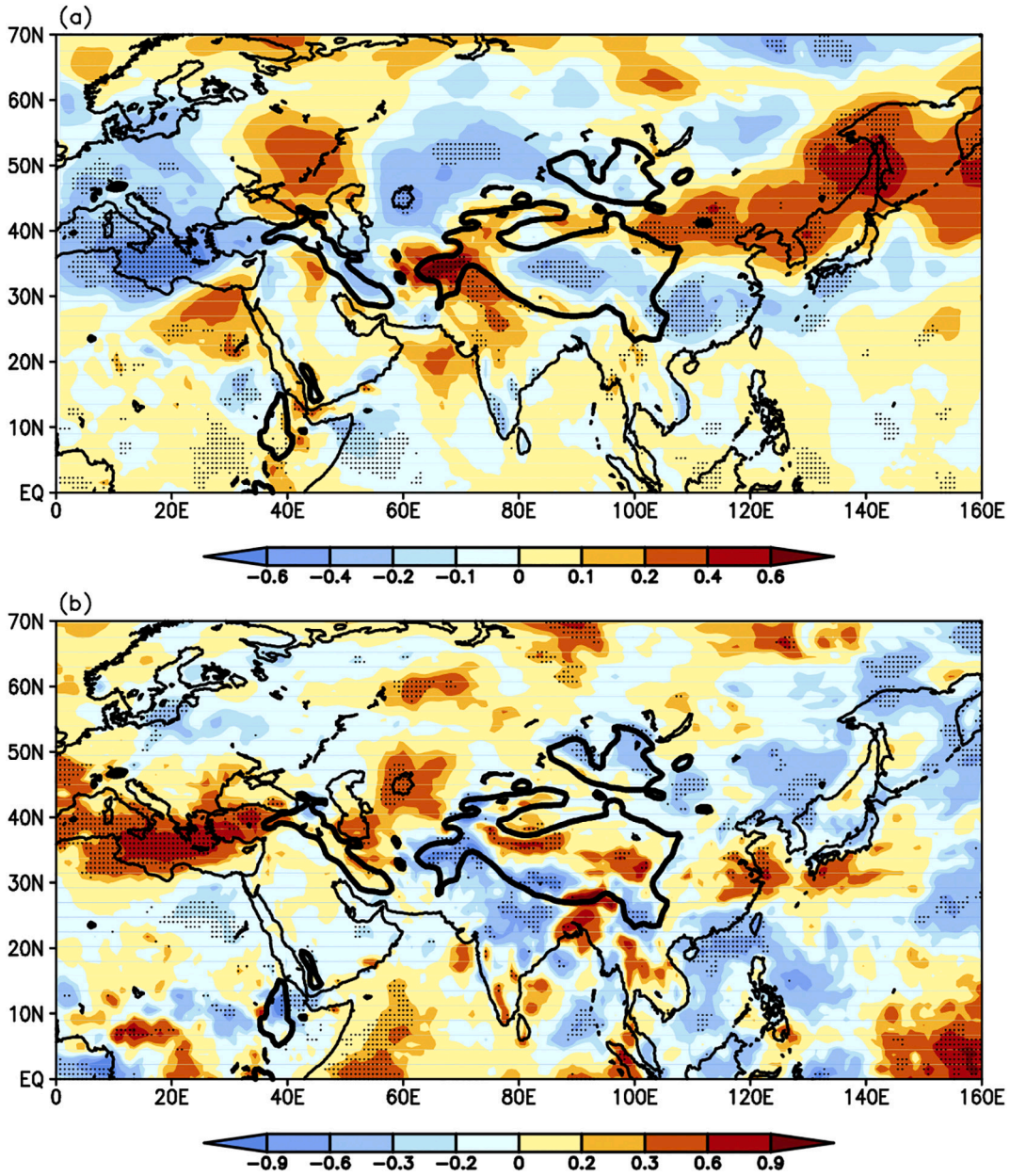

Fig. 7. Composite differences in the (a) horizontal and (b) vertical temperature advection (°C·day^{-1}) vertically integrated from the surface to 100 hPa between the high and low TTT index cases. The thick black lines represent the 1500 m topographic contour and the stippled areas are significant above the 95% confidence level.

regions. Fig. 8a shows the composite difference in the surface downward solar radiation flux between the high and low TTT index cases. Significant positive anomalies appear over East Asia (the Yangtze River–Yellow River region) and some regions of Central Asia and West Asia, indicating that more solar radiation reaches the land surface. The amounts of medium and low cloud cover decrease (Fig. 8b and c), which allows more solar radiation to warm the surface. The anomalous subsiding motion over East Asia, Central Asia and West Asia associated with the high TTT (Fig. 5) therefore contribute to the decreased amounts of medium and low cloud cover, leading to an increase in the surface incident solar radiation and the high SAT in these regions.

In general, the high SATs over West Asia and Central Asia associated with the high TTT mainly result from the increased tropospheric vertical temperature advection and surface incident solar radiation resulting from the anomalous subsiding motion. The anomalies in the tropospheric vertical temperature advection and surface incident solar radiation over East Asia resulting from the anomalous subsiding motion and the anomaly in the horizontal temperature advection due to the enhanced East Asian summer monsoon jointly lead to the high SATs at this region.

The changes in TTT therefore changes the meridional temperature gradients from the MEC to the north and south, leading to the anomalous anticyclonic circulation and anomalous subsiding motion over the mid- to high latitudes of Eurasia, an enhanced East Asian summer monsoon and the high SAT over West Asia, Central Asia, and East Asia.

Previous studies have indicated that the interannual anomaly of East Asian summer monsoon is closely related to the location and intensity of the westerly jet, in addition to the Arctic Oscillation and the sea surface temperature (Chang et al., 2000a, 2000b; Liao et al., 2004; Kuang and Zhang, 2006; Li and Pan, 2006; Xuan et al., 2011; Gong et al., 2011). We therefore investigated further the relation between the thermal condition of the Tibetan troposphere and the climate over East Asia. Fig. 9a shows the correlation map between the JJA TTT index and the precipitation at 160 stations in China. Significant positive values

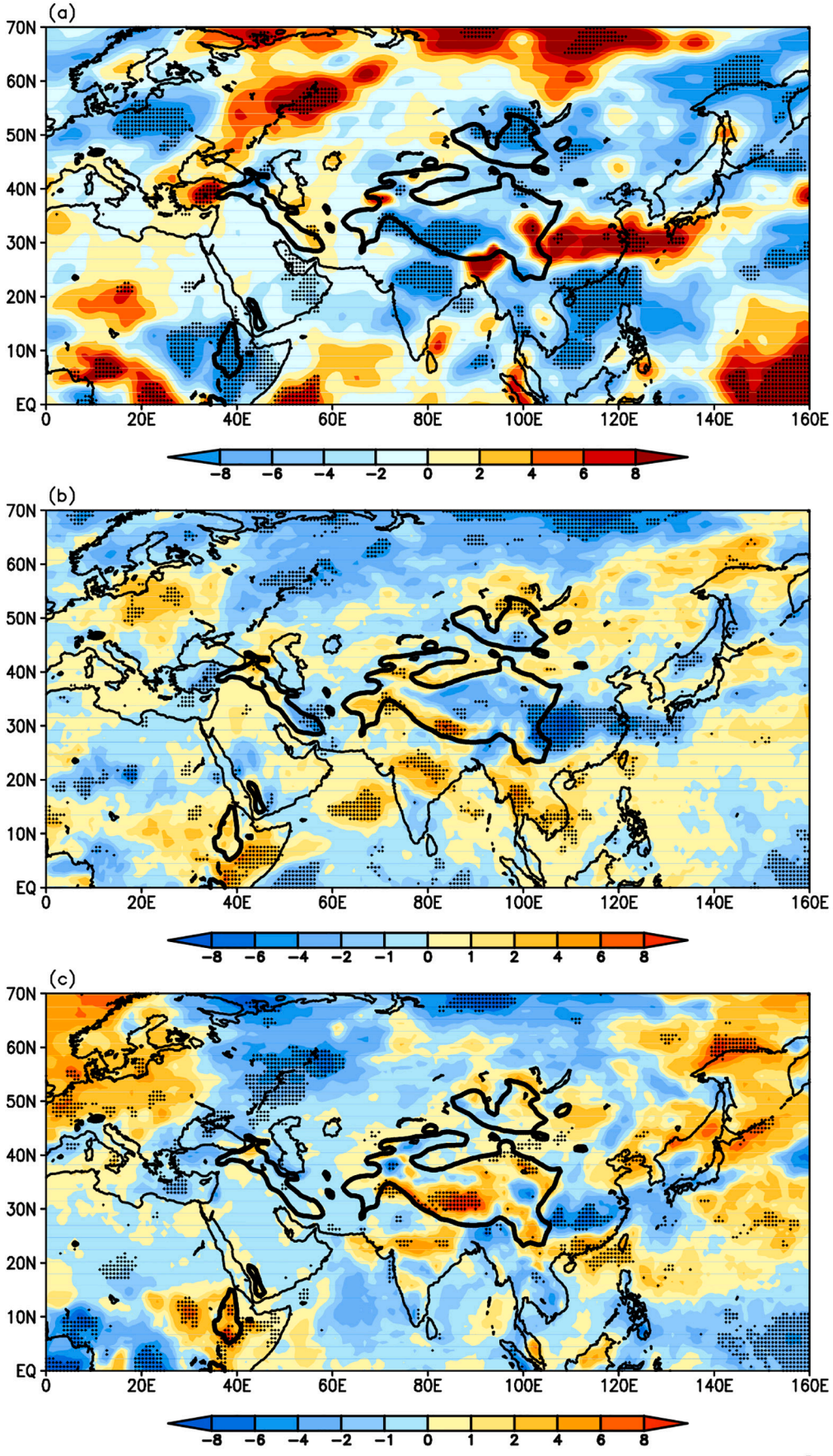

Fig. 8. Composite differences in the (a) surface downward solar radiation flux (10^{-5}·J·m^{-2}), (b) medium cloud cover (%) and (c) low cloud cover (%) between the high and low TTT index cases. The thick black lines represent the 1500 m topographic contour. The stippled areas are significant at the 90% confidence level.

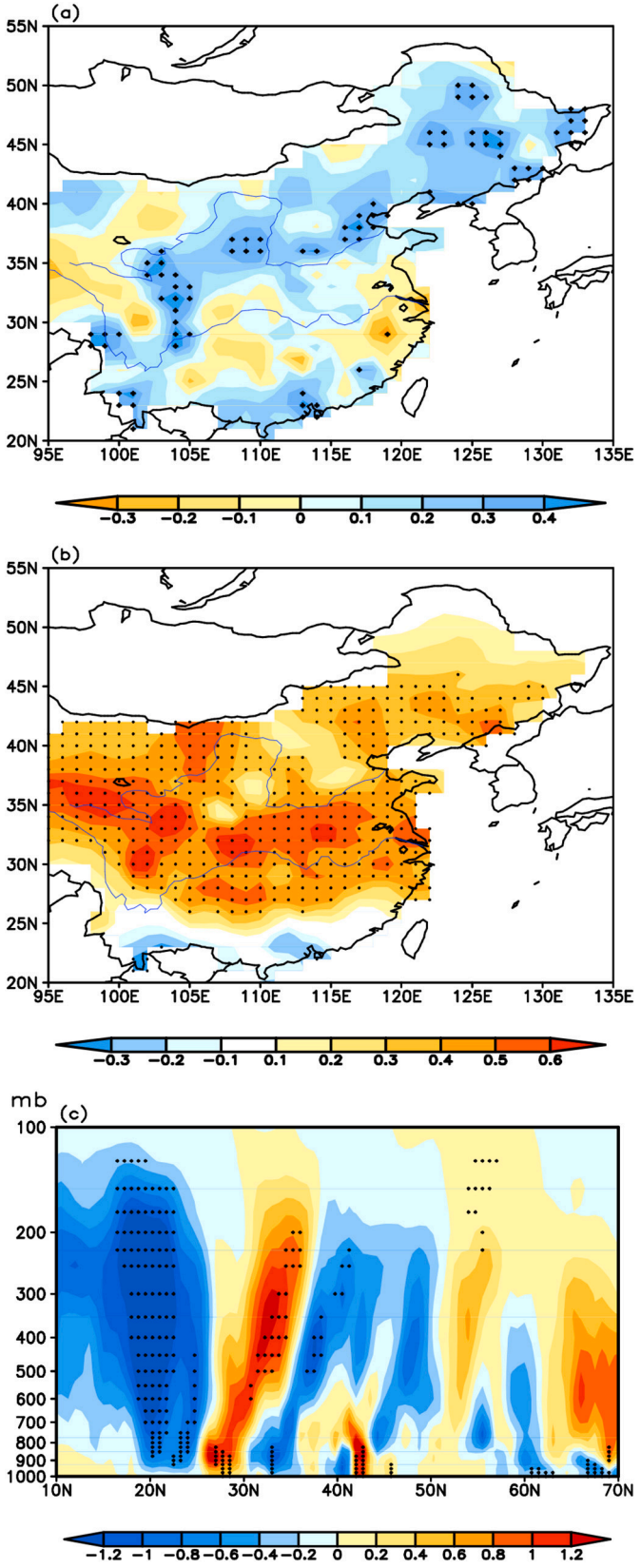

Fig. 9. (a) Map of the correlation between the JJA TTT index and the 160 station precipitation in China. (b) Map of the correlation between the JJA TTT index and the 160 station SAT in China. (c) Composite difference in the vertical velocity (10^{-2}·Pa·s^{-1}) along 110°E-120°E between the high and low TTT index cases. The stippled areas are significant above the 95% confidence level.

appear in North China and Northeast China, indicating that the increased precipitation in these regions is associated with the increased TTT. Consistent with Fig. 6, Fig. 9b shows the close relation of the TTT and the SAT in eastern China, especially over the Yangtze River–Yellow River region. Fig. 9a and b together show that when the TTT increases, precipitation in North China and Northeast China and the SAT over the Yangtze River–Yellow River region also tend to increase.

The increase in precipitation in North China and Northeast China and the SAT over the Yangtze River–Yellow River region associated with the high TTT are related to anomalies in the vertical motion over East Asia. Fig. 9c shows the composite difference in the vertical velocity along 110°E-120°E between the high and low TTT index cases. Significant positive values appear in the mid- to upper troposphere over the Yangtze River–Yellow River region, indicating the local subsiding motion anomalies, which favor an increase in the local SAT. Significant negative values appear over North China and Northeast China, indicating that the ascending motion anomalies facilitate the increase in the local precipitation. The patterns of precipitation and the atmospheric circulation over East Asia are consistent with those associated with the northward shift in the westerly jet (Xuan et al., 2011). Thus the thermal condition of the Tibetan Plateau is probably linked with the variability of the East Asian climate through the westerly jet.

These analyses show that the temperature in the mid- to upper troposphere over the Tibetan Plateau is highest at the same latitude in summer and that the variability of TTT is coincident and similar to the Eurasian tropospheric temperature on an interannual timescale. The high TTT is accompanied by an increase in the mid- to upper tropospheric temperature over the MEC. The high-temperature air leads to the anomalous southward (northward) temperature gradient to the subtropics (higher latitudes), accompanied by an anomalous easterly wind over 25°N-35°N and an anomalous westerly wind over 40°N-50°N in the mid- to upper troposphere. These features indicate the enhancement and northward shift in the Eurasian westerly jet. The anomalous anticyclonic circulation and subsiding motion appear between the anomalous easterly and westerly winds. Accordingly, the SAT increases over West Asia, Central Asia, and East Asia. The enhanced East Asian summer monsoon, associated with the high TTT, also contributes to the high SAT over East Asia via horizontal temperature advection. The northward shift in the westerly jet over East Asia is related to increased precipitation in North China and Northeast China. It is unclear whether the atmospheric circulation anomalies associated with the TTT reflect an influence of the heating anomalies over the Tibetan Plateau. The following section uses a climate model to investigate the influence of the heating anomaly over the Tibetan Plateau on the atmospheric circulation over the Eurasian continent.

4. Model results

The difference in the type of vegetation indicates a lower albedo over the Tibetan Plateau in the CAM3-tree relative to the CAM3-bare, which can change the heating effect of the Tibetan Plateau. The difference between CAM3-tree and CAM3-bare will therefore present an enhanced heating effect of the Tibetan Plateau.

Fig. 10a shows the composite difference in the vertically (500–200 hPa) averaged temperature between CAM-tree and CAM-bare. Significant positive values appear over the Eurasian continent at latitudes 25°N-45°N, with the strongest center of 1.4 °C over the Tibetan Plateau. This indicates that the increased mid- to upper tropospheric temperature over the Tibetan Plateau is forced. The longitude–height cross-section of air temperature along 30° N (Fig. 10b) shows that the influence of the heating effect of the Tibetan Plateau also stretches westward. Significant positive values appear in the mid- to upper troposphere over East Asia, the Tibetan Plateau, Central Asia and West Asia. The results imply that the anomalous temperature gradients from the MEC to the south and north are well simulated. These are consistent with the observations (Fig. 2), which demonstrates the thermal forcing

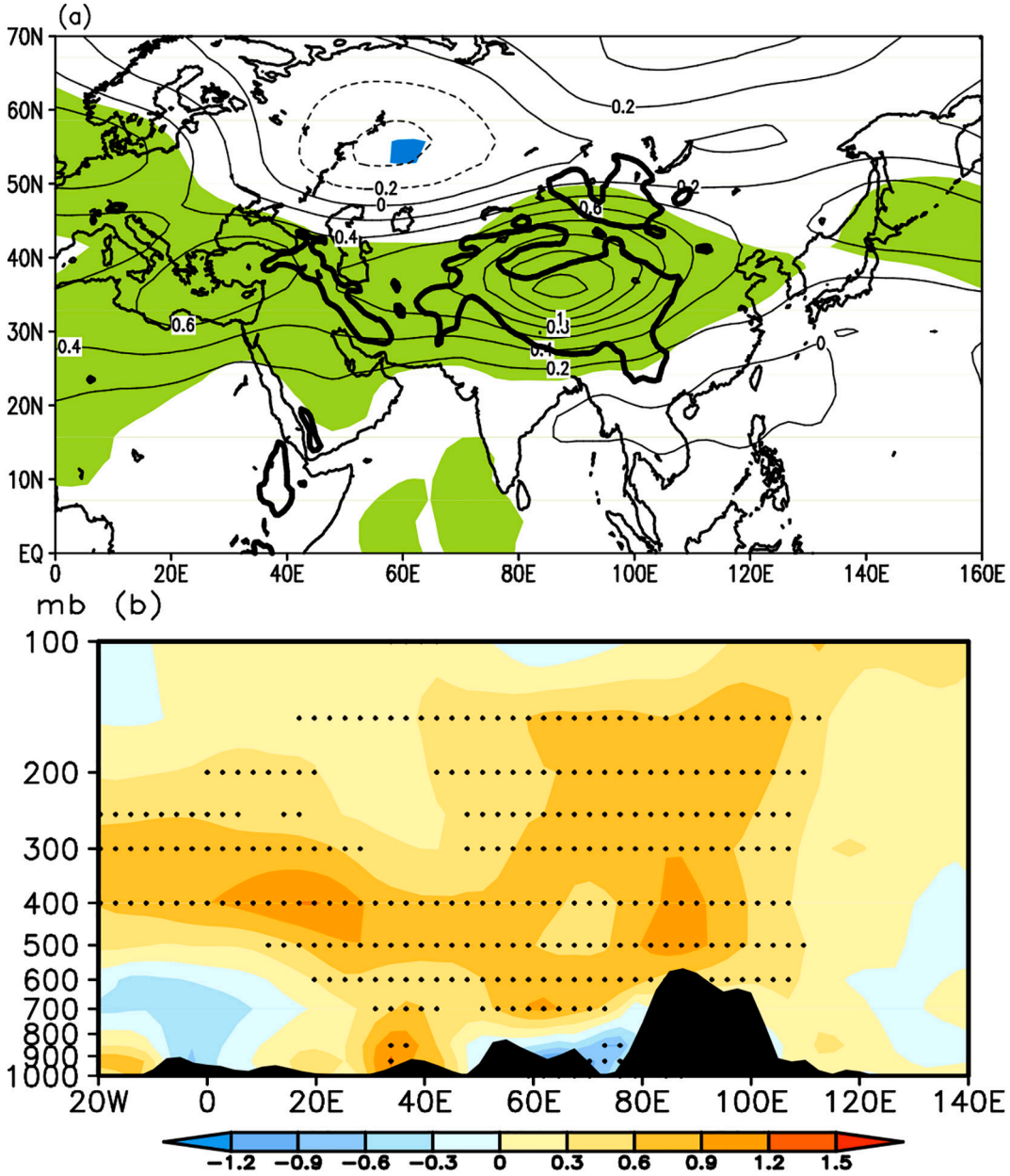

Fig. 10. Differences in air temperature (˚C) between CAM-tree and CAM-bare for (a) the vertically (500–200 hPa) averaged air temperature field and (b) the longitude–height cross-section of the air temperature along 30˚ N. The thick black lines in part (a) represent the 1500 m topographic contour. The black shaded areas in part (b) indicate the topography. The shaded areas in part (a) and the stippled areas in part (b) are significant at the 95% confidence level.

of the Tibetan Plateau on both the Eurasian tropospheric temperature and the temperature gradients from the MEC to the south and north.

Fig. 11 shows the composite differences in the zonal wind along 45°N and 30°N between CAM-tree and CAM-bare. Significant positive and negative values appear in the mid- to upper troposphere along 45°N and 30°N, respectively, which are generally similar to those in Fig. 3b and c and indicate the northward shift in the Eurasian westerly jet in CAM-tree relative to CAM-bare. Fig. 12 shows the composite difference in the horizontal wind fields between CAM-tree and CAM-bare. In the mid- to upper troposphere (Fig. 12a and b), anomalous westerly and easterly winds appear at mid- to high latitudes (40°N-50°N) and at mid- to lower latitudes (30°N-40°N), respectively, which further supports the enhancement and northward shift of the Eurasian westerly jet. Between the anomalous westerly and easterly winds, anomalous anticyclonic circulation occurs over West Asia, Central Asia, and East Asia. Southerly wind anomalies in the lower troposphere (Fig. 12c) prevail from South China to Northeast China, indicating an enhanced East Asian summer monsoon. These simulated results are similar to the observations (Figs. 3 and 4), showing the impact of the increased heating effect of the Tibetan Plateau on the enhancement and northward shift in the Eurasian westerly jet, the anticyclonic circulation anomalies over mid-latitudes over the Eurasian continent and the enhancement of the East Asian summer monsoon.

The anomalous upward motion over East Asia appears between 35°N-50°N in the mid- to upper troposphere (Fig. 13c), consistent with observations (Fig. 9c). Anomalous subsiding motion appears over southern China (Fig. 13c), but is not significant. Corresponding to the anomalous vertical motion, the model successfully simulates the increase in precipitation over North China and Northeast Asia (Fig. 13a). The area of the simulated positive precipitation anomaly extends to the Yangtze River–Yellow River region—that is, wider than the observed anomaly. The increased precipitation in the Yangtze River–Yellow

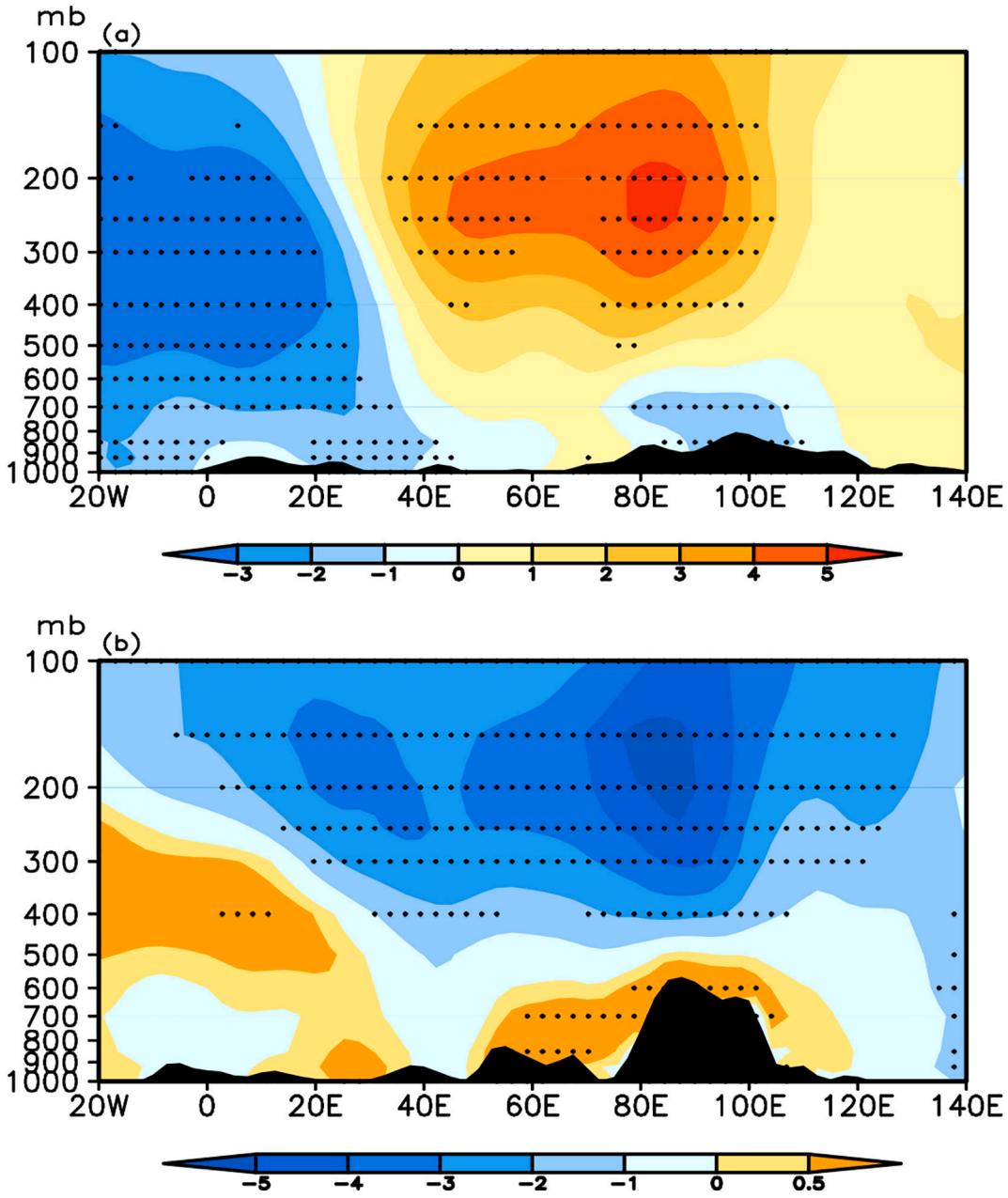

Fig. 11. Differences in the zonal winds ($m \cdot s^{-1}$) along (a) 45° N and (b) 30° N between CAM-tree and CAM-bare. The black shaded areas indicate the topography and the stippled areas are significant above the 95% confidence level.

River region cools the atmosphere and therefore the simulated positive precipitation anomaly in the Yangtze River–Yellow River region is incorrect and may lead to failure of the SAT simulation (Fig. 13b).

Enhanced heating over the Tibetan Plateau therefore triggers the increase in tropospheric temperature over the MEC, the anomalous temperature gradient from the MEC to its two flanks, the enhancement and northward shift in the Eurasian westerly jet, the anomalous anticyclonic circulation in the mid- to upper troposphere over West Asia, Central Asia, and East Asia, the enhancement of the East Asian summer monsoon, and the anomalous upward motion over North China and Northeast China.

5. Summary and discussion

5.1. Summary

Using the monthly data from ERA-Interim database, SAT data from GISS, and SAT and precipitation from 160 stations in China for the time period 1979–2018, we investigated the temporal variation in the summer TTT, its relation with the tropospheric temperature over Eurasia and its linkage with the Eurasian atmospheric circulation and climate anomalies. The TTT is higher than the tropospheric temperature in other regions at the same latitude and the tropospheric temperature over the MEC increases in association with the high TTT. The increase in TTT leads to anomalous gradients in the tropospheric temperature from the MEC to its two flanks and anomalous westerly and easterly winds on its northern and southern flanks, respectively, in the mid- to upper troposphere. Anomalous anticyclonic circulation and subsiding

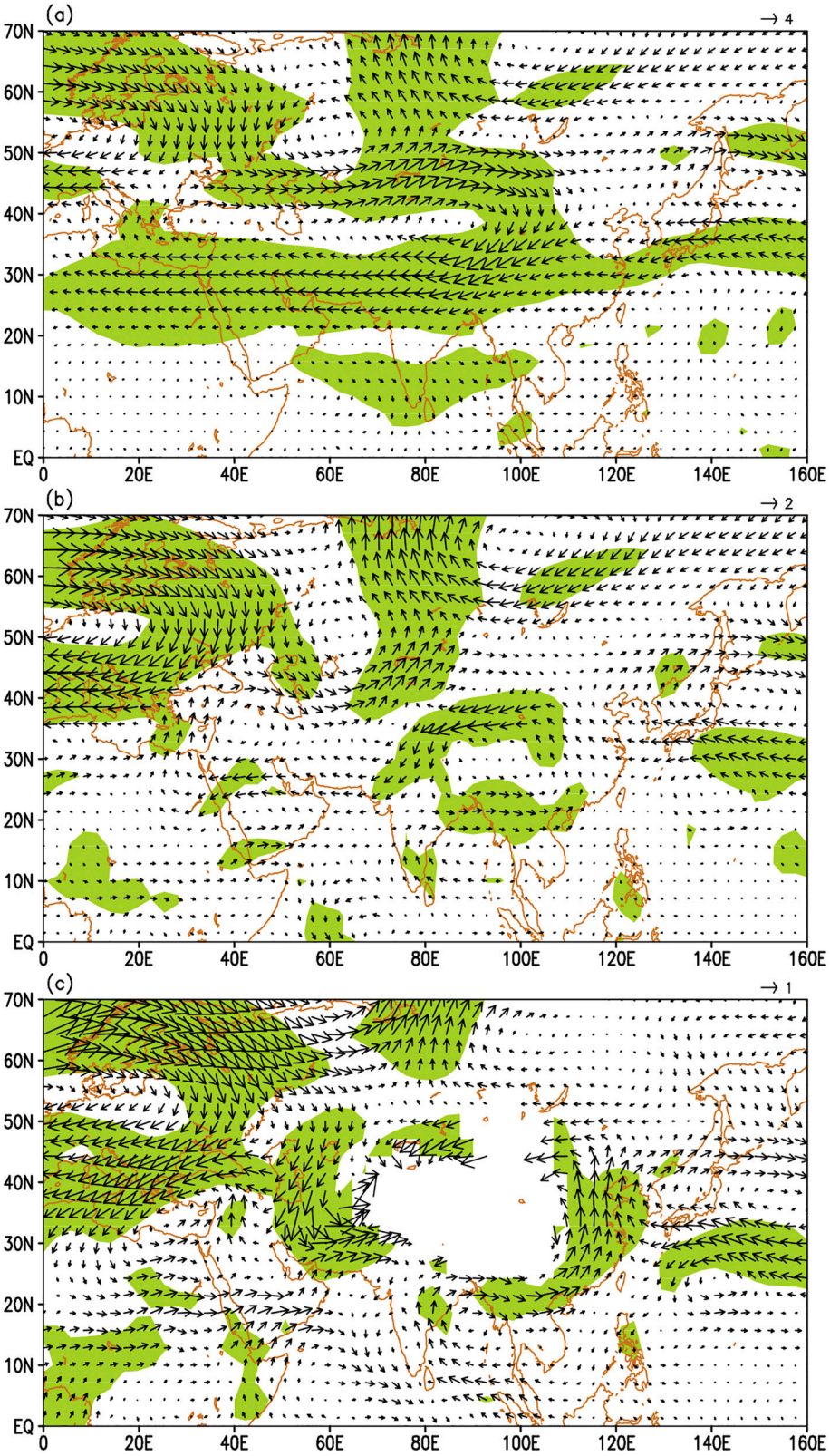

Fig. 12. Differences in the (a) 200, (b) 500 and (c) 850 hPa horizontal wind vectors ($m \cdot s^{-1}$) between CAM-tree and CAM-bare. The shaded areas are significant at the 95% confidence level. The white areas over land in part (c) are the regions below the surface.

motion appear between the anomalous westerly and easterly winds, with centers in West Asia, Central Asia, and East Asia. These features contribute to the high SAT in these regions via the anomalous vertical temperature advection in the troposphere and the surface incident solar radiation. The enhanced East Asian summer monsoon in association with the high TTT also contributes to the high SAT over East Asia via horizontal temperature advection. The westerly wind anomalies in the mid- to upper troposphere over the MEC indicate the northward shift in

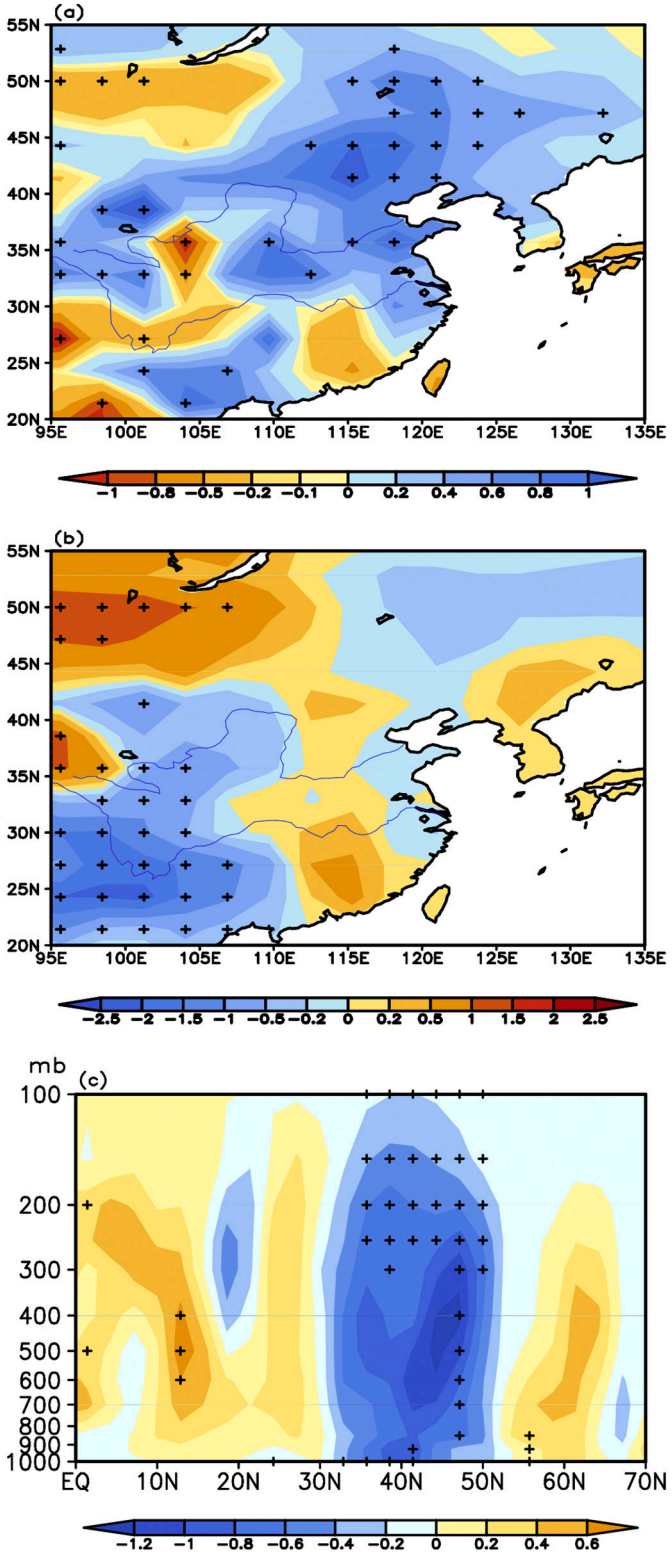

Fig. 13. Differences in (a) precipitation (mm·day^{-1}), (b) SAT (°C) and (c) vertical velocity (10^{-2}·Pa·s^{-1}) along 110°E-120°E between CAM-tree and CAM-bare. The stippled areas are significant above the 90% confidence level.

the mid-latitude westerly jet, which is related to the anomalous upward motion and higher than normal precipitation in Northeast China and North China.

We carried out sensitivity experiments using an atmospheric model with a prescribed sea surface temperature scheme, in which the tropospheric heating over the Tibetan Plateau was changed by adjusting the type of surface vegetation. These experiments also showed the consistency of the thermal conditions of the troposphere over the Tibetan Plateau and the MEC and their impact on the anomalous easterly winds in the south of the MEC, the anomalous westerly winds to the north of the MEC, the anomalous anticyclonic circulation and subsiding motion at the mid- to upper troposphere over West Asia and Central Asia and East Asia, the enhancement and northward shift in the Eurasian westerly jet, the enhancement of the East Asian summer monsoon and the increased precipitation over North China and Northeast China. These results suggest that anomalous tropospheric heating over the Tibetan Plateau in summer can affect the atmospheric circulation and climate over the Eurasian continent.

5.2. Discussion

Zhao et al. (2014) showed that the change in tropospheric temperature over Central Asia can also affect the meridional displacement of the subtropical westerly jet over western and central Asia. It has a significant correlation coefficient of 0.42 (> 99% confidence level) with the original JJA TTT index (not detrended). The original TTT index (not detrended) shows a significant upward trend. However, the tropospheric temperature over Central Asia did not show a significant downward or upward trend during the time period 1979–2018. Therefore their high correlation implies that the interannual variability of the TTT is consistent with that over Central Asia. Nevertheless, the trends in tropospheric temperature vary with the regions of the Eurasian continent.

The Tibetan Plateau is a source of heat in summer and is located in the region of anomalous easterly winds associated with the high TTT (Fig. 4a and b). Anomalous anticyclonic (cyclonic) circulations appear to the north (south), in a similar pattern to the model of Gill (1980). The typical Gill model is the response to symmetrical heating at the surface of a tropical ocean. The Tibetan Plateau is located in the northern hemisphere and supplies heat to the atmosphere in the mid- to upper troposphere. Further investigations are required to determine whether heating by the Tibetan Plateau obeys the Gill theory.

Declaration of Competing Interest

The authors declare that they have no known competing financial interests or personal relationships that could have appeared to influence the work reported in this paper.

Acknowledgements

We thank the ECMWF for providing the ERA-Interim data, and the NOAA/OAR/ESRL PSD for providing the GISS air temperature. This work was jointly sponsored by the Strategic Priority Research Program of Chinese Academy of Sciences (XDA20100300), Key Special Projects of National Key R&D Program of China (2018YFC1505706), the National Natural Science Foundation of China (41775084), and the Basic Research Special Project of Chinese Academy of Meteorological Sciences (2019Z008).

References

Branstator, G., 2002. Circumglobal teleconnections, the jet stream waveguide, and the North Atlantic oscillation. J. Clim. 15 (14), 1893–1910. https://doi.org/10.1175/1520-0442(2002)015<1893:cttjsw>2.0.co;2.

Cai, D., Fraedrich, K., Sielmann, F., Guan, Y., Guo, S., Zhang, L., Zhu, X., 2014. Climate and vegetation: an ERA-interim and GIMMS NDVI analysis. J. Clim. 27 (13), 5111–5118.

Cai, D., Fraedrich, K., Sielmann, F., Zhang, L., Zhu, X., Guo, S., Guan, Y., 2015. Vegetation dynamics on the Tibetan Plateau (1982–2006): an attribution by ecohydrological diagnostics. J. Clim. 28 (11), 4576–4584.

Chang, C.P., Zhang, Y., Li, T., 2000a. Interannual and interdecadal variations of the East Asian summer monsoon and tropical Pacific SSTs. PartIRoles of the Subtropical

Ridge. J. Clim. 13 (24), 4310–4325.
Chang, C.P., Zhang, Y., Li, T., 2000b. Interannual and interdecadal variations of the East Asian summer monsoon and tropical Pacific SSTs. PartII: meridional structure of the monsoon. J. Clim. 13 (24), 4326–4340.
Chen, L., Wu, R., 2000. Interannual and decadal variations of snow cover over Qinghai-Xizang Plateau and their relationships to summer monsoon rainfall in China. Adv. Atmos. Sci. 17, 18–30. https://doi.org/10.1007/s00376-000-0040-7.
Collins, W.D., Rasch, P.J., Boville, B.A., Hack, J.J., McCaa, J.R., Williamson, D.L., Kiehl, J.T., Briegleb, B., Bitz, C., Lin, S.-J., Zhang, M., Dai, Y., 2004. Description of the NCAR Community Atmosphere Model (CAM 3.0). Technical Report NCAR/TN-464+STR. National Center for Atmospheric Research, Boulder, CO, pp. 226.
Drouard, M., Woollings, T., 2018. Contrasting mechanisms of summer blocking over Western Eurasia. Geophys. Res. Lett. 45 (21), 12040–12048. https://doi.org/10.1029/2018gl079894.
Duan, A.M., Wu, G.X., 2005. Role of the Tibetan Plateau thermal forcing in the summer climate patterns over subtropical Asia. Clim. Dyn. 24 (7–8), 793–807. https://doi.org/10.1007/s00382-004-0488-8.
Galarneau, T.J., Hamill, T.M., Dole, R.M., Perlwitz, J., 2012. A multiscale analysis of the extreme weather events over Western Russia and Northern Pakistan during July 2010. Mon. Weather Rev. 140 (5), 1639–1664. https://doi.org/10.1175/mwr-d-11-00191.1.
Gill, A.E., 1980. Some simple solutions for heat-induced tropical circulation. Quart. J. R. Met. Soc. 106, 447–462.
Gong, D.Y., Yang, J., Kim, S.J., Gao, Y., Guo, D., Zhou, T., Hu, M., 2011. Spring Arctic Oscillation-East Asian summer monsoon connection through circulation changes over the western North Pacific. Clim. Dyn. 37, 2199–2216.
Kuang, X., Zhang, Y., 2005. Seasonal variation of the East Asian subtropical westerly jet and its association with the heating field over East Asia. Adv. Atmos. Sci. 22 (6), 831–840.
Kuang, X., Zhang, Y., 2006. Impact of the position abnormalities of East Asian subtropical westerly jet on summer precipitation in middle lower reaches of Yangtze River (in Chinese). Plateau Meteor. 25, 382–389.
Li, C., Pan, J., 2006. Atmospheric circulation characteristics associated with the onset of Asian summer monsoon. Adv. Atmos. Sci. 23 (6), 925–939. https://doi.org/10.1007/s00376-006-0925-1.
Liao, Q., Gao, S., Wang, H., Tao, S., 2004. Interannual variation of summer subtropical westerly jet in East Asia and its impacts on the climate anomalies of East Asia summer monsoon (in Chinese). Chin. J. Geophys. 47, 12–21. https://doi.org/10.1002/cjg2.449.
Lin, H., Wu, Z., 2011. Contribution of the Autumn Tibetan Plateau snow cover to seasonal prediction of North American winter temperature. J. Clim. 24 (11), 2801–2813. https://doi.org/10.1175/2010jcli3889.1.
Liu, Y.M., Wu, G.X., Liu, H., Liu, P., 2001. Condensation heating of the Asian summer monsoon and the subtropical anticyclone in Eastern Hemisphere. Clim. Dyn. 17, 327–338. https://doi.org/10.1007/s003820000117.
Liu, Y.M., Wu, G.X., Ren, R., 2004. Relationship between the subtropical anticyclone and diabatic heating. J. Clim. 17, 682–698. https://doi.org/10.1175/1520-0442(2004)017,0682:RBTSAA.2.0. CO;2.
Lu, M., Yang, S., Li, Z., He, B., He, S., Wang, Z., 2018. Possible effect of the Tibetan Plateau on the “upstream” climate over West Asia, North Africa, South Europe and the North Atlantic. Clim. Dyn. 51 (4), 1485–1498. https://doi.org/10.1007/s00382-017-3966-5.
Luo, H., Yanai, M., 1984. The large-scale circulation and heat sources over the Tibetan Plateau and Surrounding areas during the early Summer of 1979. Part II: heat and moisture budgets. Mon. Weather Rev. 112 (5) 996–989.
Namias, J., 1991. Spring and summer 1988 drought over the contiguous United States—causes and prediction. J. Clim. 4, 54–65.
Nan, S., Zhao, P., Yang, S., Chen, J., 2009. Springtime tropospheric temperature over the Tibetan Plateau and evolutions of the tropical Pacific SST. J. Geophys. Res. 114 (D10104). https://doi.org/10.1029/2008JD011559.
Nan, S., Zhao, P., Chen, J., 2019. Variability of summertime Tibetan tropospheric temperature and associated precipitation anomalies over the Central-Eastern Sahel. Clim. Dyn. 52 (3–4), 1819–1835. https://doi.org/10.1007/s00382-018-4246-8.
Ose, T., 1996. The comparison of the simulated response to the regional snow mass anomalies over Tibet, Eastern Europe, and Siberia. J Meteor Soc Jpn. 74, 845–866.
Qin, D., Liu, S., Li, P., 2006. Snow cover distribution, variability, and response to climate change in western China. J. Clim. 19, 1820–1833. https://doi.org/10.1175/JCLI3694.1.
Robock, A., Mu, M.Q., Vinnikov, K., Robinson, D., 2003. Land surface conditions over Eurasia and Indian summer monsoon rainfall. J. Geophys. Res.-Atmos. 108 (D4). https://doi.org/10.1029/2002jd002286.
Simmons, A., Uppala, S., Dee, D., Kobayashi, S., 2007. ERA Interim: New ECMWF re-analysis products from 1989 onwards. ECMWF Newsl 110, 25–35.
Wang, C., Yang, K., Li, Y., Wu, D., Bo, Y., 2017. Impacts of spatiotemporal anomalies of Tibetan Plateau snow cover on summer precipitation in Eastern China. J. Clim. 30, 885–903.
Wu, T.W., Qian, Z.A., 2003. The relation between the Tibetan winter snow and the Asian summer monsoon and rainfall: an observational investigation. J. Clim. 16, 2038–2051. https://doi.org/10.1175/1520-0442(2003)016,2038:TRBTTW.2.0.CO;2.
Wu, G.X., Li, W.P., Guo, H., 1997. Sensible heat driven air-pump over the Tibetan Plateau and its impacts on the Asian summer monsoon. In: Ye, D.Z. (Ed.), Collections on the Memory of Zhao Jiuzhang. Science Press, Beijing, pp. 116–126.
Wu, Z., Zhang, P., Chen, H., Li, Y., 2016. Can the Tibetan Plateau snow cover influence the interannual variations of Eurasian heat wave frequency? Clim. Dyn. 46 (11 − 12), 3405–3417. https://doi.org/10.1007/s00382-015-2775-y.
Xuan, S., Zhang, Q., Sun, S., 2011. Anomalous midsummer rainfall in Yangtze River-Huaihe River valleys and its association with the East Asia westerly jet. Adv. Atmos. Sci. 28 (2), 387–397. https://doi.org/10.1007/s00376-010-0111-3.
Yanai, M., Li, C., Song, Z., 1992. Seasonal heating of the Tibetan Plateau and its effects on the evolution of the Asian summer monsoon. Journal of the Meteorological Society of Japan. Ser. II 70 (1B), 319–351. https://doi.org/10.2151/jmsj1965.70.1B_319.
Ye, D.Z., Gao, Y.X., 1979. The Meteorology of the Qinghai-Xizang (Tibet) Plateau. Science Press, Beijing, pp. 1–278 (in Chinese).
Yeh, T.C., 1950. The Circulation of the high troposphere over China in the Winter of 1945–46. Tellus. 2, 173–183.
Zhang, Y.S., Li, T., Wang, B., 2004. Decadal change of the spring snow depth over the Tibetan Plateau: the associated circulation and influence on the East Asian summer monsoon. J. Clim. 17 (14), 2780–2793. https://doi.org/10.1175/1520-0442(2004)017<2780:dcotss>2.0.co.2.
Zhang, Y., Kuang, X., Guo, W., Zhou, T., 2006. Seasonal evolution of the upper-tropospheric westerly jet core over East Asia. Geophys. Res. Lett. 33 (11). https://doi.org/10.1029/2006gl026377.
Zhang, Y., Yan, P., Liao, Z., Huang, D., Zhang, Y., 2019. The winter concurrent meridional shift of the East Asian jet streams and the associated thermal conditions. J. Clim. 32 (7), 2075–2088. https://doi.org/10.1175/jcli-d-18-0085.1.
Zhao, P., Zhou, Z., Liu, J., 2007. Variability of Tibetan spring snow and its associations with the hemispheric extratropical circulation and East Asian summer monsoon rainfall: an observational investigation. J. Clim. 20 (15), 3942–3955. https://doi.org/10.1175/jcli4205.1.
Zhao, P., Cao, Z.H., Chen, J.M., 2010. A summer teleconnection pattern over the extra-tropical Northern Hemisphere and associated mechanisms. Clim. Dyn. 35, 523–534. https://doi.org/10.1007/s00382-009-0699.
Zhao, P., Yang, S., Wu, R., Wen, Z., Chen, J., Wang, H., 2012. Asian origin of interannual variations of summer climate over the extratropical North Atlantic Ocean. J. Clim. 25 (19), 6594–6609. https://doi.org/10.1175/jcli-d-11-00617.1.
Zhao, Y., Huang, A., Zhou, Y., Huang, D., Yang, Q., et al., 2014. Impact of the middle and upper tropospheric cooling over Central Asia on the summer rainfall in the Tarim Basin, China. J. Clim. 27 (12), 4721–4732. https://doi.org/10.1175/jcli-d-13-00456.1.
Zhu, Y., Liu, H., Ding, Y., Zhang, F., Li, W., 2015. Interdecadal variation of spring snow depth over the Tibetan Plateau and its influence on summer rainfall over East China in the recent 30 years. Int. J. Climatol. 35 (12), 3654–3660. https://doi.org/10.1002/joc.4239.